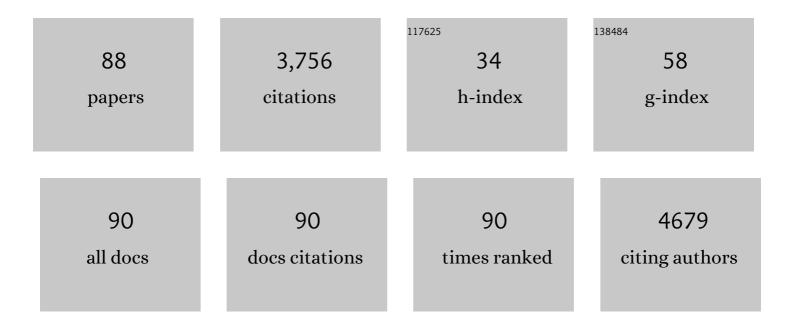
List of Publications by Year in descending order

Source: https://exaly.com/author-pdf/7427067/publications.pdf Version: 2024-02-01



#	Article	IF	CITATIONS
1	Recent advances in functional mesoporous graphitic carbon nitride (mpg-C ₃ N ₄) polymers. Nanoscale, 2017, 9, 10544-10578.	5.6	189
2	Cuprous oxide (Cu2O) crystals with tailored architectures: A comprehensive review on synthesis, fundamental properties, functional modifications and applications. Progress in Materials Science, 2018, 96, 111-173.	32.8	183
3	Recent advances in hybrid Cu ₂ O-based heterogeneous nanostructures. Nanoscale, 2015, 7, 10850-10882.	5.6	157
4	Diversified copper sulfide (Cu _{2â^'x} S) micro-/nanostructures: a comprehensive review on synthesis, modifications and applications. Nanoscale, 2017, 9, 11357-11404.	5.6	154
5	Hierarchical CuO nanoflowers: water-required synthesis and their application in a nonenzymatic glucose biosensor. Physical Chemistry Chemical Physics, 2013, 15, 10904.	2.8	125
6	Facile Water-Assisted Synthesis of Cupric Oxide Nanourchins and Their Application as Nonenzymatic Glucose Biosensor. ACS Applied Materials & Interfaces, 2013, 5, 4429-4437.	8.0	117
7	Amorphous TiO ₂ nanostructures: synthesis, fundamental properties and photocatalytic applications. Catalysis Science and Technology, 2019, 9, 4198-4215.	4.1	105
8	The crystal-facet-dependent effect of polyhedral Cu2O microcrystals on photocatalytic activity. Catalysis Science and Technology, 2012, 2, 925.	4.1	99
9	Recent advances in tuning crystal facets of polyhedral cuprous oxide architectures. RSC Advances, 2014, 4, 3804-3822.	3.6	89
10	Templating synthesis of hollow CuO polyhedron and its application for nonenzymatic glucose detection. Journal of Materials Chemistry A, 2014, 2, 7306-7312.	10.3	87
11	Morphological zinc stannate: synthesis, fundamental properties and applications. Journal of Materials Chemistry A, 2017, 5, 20534-20560.	10.3	85
12	Nanoparticle-aggregated CuO nanoellipsoids for high-performance non-enzymatic glucose detection. Journal of Materials Chemistry A, 2014, 2, 10073.	10.3	80
13	Cu2O-templated strategy for synthesis of definable hollow architectures. Chemical Communications, 2014, 50, 7403.	4.1	80
14	Template-Free Synthesis of Well-Defined Truncated Edge Polyhedral Cu ₂ O Architectures. Crystal Growth and Design, 2010, 10, 541-547.	3.0	75
15	Highly symmetric polyhedral Cu2O crystals with controllable-index planes. CrystEngComm, 2011, 13, 2217.	2.6	75
16	Mesocrystals for photocatalysis: a comprehensive review on synthesis engineering and functional modifications. Nanoscale Advances, 2019, 1, 34-63.	4.6	75
17	High-index faceted metal oxide micro-/nanostructures: a review on their characterization, synthesis and applications. Nanoscale, 2019, 11, 15739-15762.	5.6	74
18	Simultaneously engineering K-doping and exfoliation into graphitic carbon nitride (g-C3N4) for enhanced photocatalytic hydrogen production. International Journal of Hydrogen Energy, 2019, 44, 778-787.	7.1	71

#	Article	IF	CITATIONS
19	Surfactant-free CuO mesocrystals with controllable dimensions: green ordered-aggregation-driven synthesis, formation mechanism and their photochemical performances. CrystEngComm, 2013, 15, 867-877.	2.6	67
20	Cu ₂ O Template Strategy for the Synthesis of Structure-Definable Noble Metal Alloy Mesocages. Crystal Growth and Design, 2011, 11, 3694-3697.	3.0	61
21	Synthesis, Functional Modifications, and Diversified Applications of Hybrid BiOCl-Based Heterogeneous Photocatalysts: A Review. Crystal Growth and Design, 2021, 21, 6576-6618.	3.0	61
22	Synthesis, Functional Modifications, and Diversified Applications of Molybdenum Oxides Micro-/Nanocrystals: A Review. Crystal Growth and Design, 2018, 18, 6326-6369.	3.0	60
23	Facile constructing of isotype g-C3N4(bulk)/g-C3N4(nanosheet) heterojunctions through thermal polymerization of single-source glucose-modified melamine: An efficient charge separation system for photocatalytic hydrogen production. Applied Surface Science, 2020, 500, 143985.	6.1	58
24	Bottom-up assembly of hierarchical Cu2O nanospheres: controllable synthesis, formation mechanism and enhanced photochemical activities. CrystEngComm, 2012, 14, 3545.	2.6	54
25	Facet-selective growth of Cu–Cu ₂ O heterogeneous architectures. CrystEngComm, 2012, 14, 40-43.	2.6	54
26	Constructing oxygen-doped g-C ₃ N ₄ nanosheets with an enlarged conductive band edge for enhanced visible-light-driven hydrogen evolution. Inorganic Chemistry Frontiers, 2018, 5, 1721-1727.	6.0	54
27	Constructing the Z-scheme TiO2/Au/BiOI nanocomposite for enhanced photocatalytic nitrogen fixation. Applied Surface Science, 2021, 556, 149785.	6.1	54
28	Facet Junction Engineering for Photocatalysis: A Comprehensive Review on Elementary Knowledge, Facet‧ynergistic Mechanisms, Functional Modifications, and Future Perspectives. Advanced Functional Materials, 2022, 32, 2106982.	14.9	51
29	Nanoporous copper oxide ribbon assembly of free-standing nanoneedles as biosensors for glucose. Analyst, The, 2015, 140, 5205-5215.	3.5	49
30	One-pot construction of Ta-doped BiOCl/Bi heterostructures toward simultaneously promoting visible light harvesting and charge separation for highly enhanced photocatalytic activity. Applied Surface Science, 2021, 543, 148798.	6.1	49
31	Mesoporous graphitic carbon nitride (g-C ₃ N ₄) nanosheets synthesized from carbonated beverage-reformed commercial melamine for enhanced photocatalytic hydrogen evolution. Materials Chemistry Frontiers, 2019, 3, 597-605.	5.9	44
32	Unique polyhedral 26-facet CuS hollow architectures decorated with nanotwinned, mesostructural and single crystalline shells. CrystEngComm, 2011, 13, 6200.	2.6	39
33	Etching-limited branching growth of cuprous oxide during ethanol-assisted solution synthesis. CrystEngComm, 2011, 13, 2837.	2.6	39
34	A facile strategy for the synthesis of hierarchical CuO nanourchins and their application as non-enzymatic glucose sensors. RSC Advances, 2013, 3, 13712.	3.6	39
35	Twins in polyhedral 26-facet Cu7S4 cages: Synthesis, characterization and their enhancing photochemical activities. Dalton Transactions, 2012, 41, 3214.	3.3	35
36	Copper sulfide cages wholly exposed with nanotwinned building blocks. CrystEngComm, 2012, 14, 67-70.	2.6	34

#	Article	IF	CITATIONS
37	Facile construction of nickel-doped hierarchical BiOCl architectures for enhanced visible-light-driven photocatalytic activities. Materials Research Bulletin, 2021, 138, 111208.	5.2	34
38	Organic dye-reformed construction of porous-defect g-C3N4 nanosheet for improved visible-light-driven photocatalytic activity. Applied Surface Science, 2021, 568, 150986.	6.1	33
39	Selective-etching growth of urchin-like Cu2O architectures. CrystEngComm, 2011, 13, 6616.	2.6	31
40	A ternary photocatalyst of all-solid-state Z-scheme TiO2–Au–BiOBr for efficiently degrading various dyes. Journal of Alloys and Compounds, 2020, 839, 155597.	5.5	31
41	Facile hydroxyl-assisted synthesis of morphological Cu ₂ O architectures and their shape-dependent photocatalytic performances. New Journal of Chemistry, 2014, 38, 4656-4660.	2.8	30
42	Novel cone-like ZnO mesocrystals with co-exposed (101̄1) and (0001̄) facets and enhanced photocatalytic activity. Inorganic Chemistry Frontiers, 2018, 5, 2257-2267.	6.0	30
43	In-situ construction of direct Z-scheme sea-urchin-like ZnS/SnO2 heterojunctions for boosted photocatalytic hydrogen production. International Journal of Hydrogen Energy, 2022, 47, 9201-9208.	7.1	30
44	Seed-mediated synthesis of polyhedral 50-facet Cu2O architectures. CrystEngComm, 2011, 13, 5993.	2.6	29
45	Identification of the Miller indices of a crystallographic plane: a tutorial and a comprehensive review on fundamental theory, universal methods based on different case studies and matters needing attention. Nanoscale, 2020, 12, 16657-16677.	5.6	29
46	A surfactant-free strategy for controllable growth of hierarchical copper oxide nanostructures. CrystEngComm, 2013, 15, 5275.	2.6	27
47	Unusual Designated-Tailoring on Zone-Axis Preferential Growth of Surfactant-Free ZnO Mesocrystals. Crystal Growth and Design, 2012, 12, 2411-2418.	3.0	26
48	Nanotwins in polycrystalline Cu7S4 cages: highly active architectures for enhancing photocatalytic activities. Catalysis Science and Technology, 2012, 2, 1309.	4.1	25
49	Elucidating a twin-dependent chemical activity of hierarchical copper sulfide nanocages. Physical Chemistry Chemical Physics, 2013, 15, 15964.	2.8	25
50	Purposefully designing novel hydroxylated and carbonylated melamine towards the synthesis of targeted porous oxygen-doped g-C ₃ N ₄ nanosheets for highly enhanced photocatalytic hydrogen production. Catalysis Science and Technology, 2019, 9, 5150-5159.	4.1	25
51	Mechanism Insight into an Unprecedented Dual Seriesâ€Parallel Photocharge Separation in Quaternary Cu ₂ O Facet Junctions. Advanced Functional Materials, 2022, 32, .	14.9	24
52	One-pot integration of S-doped BiOCl and ZnO into type-II photocatalysts: Simultaneously boosting bulk and surface charge separation for enhanced antibiotic removal. Separation and Purification Technology, 2022, 299, 121725.	7.9	24
53	Nanoparticle-aggregated paddy-like copper dendritic nanostructures. CrystEngComm, 2011, 13, 1916-1921.	2.6	23
54	Nanoparticle-aggregated hollow copper microcages and their surface-enhanced Raman scattering activity. CrystEngComm, 2013, 15, 6136.	2.6	23

#	Article	IF	CITATIONS
55	Polyhedron-aggregated multi-facet Cu2O homogeneous structures. CrystEngComm, 2011, 13, 6040.	2.6	22
56	Unprecedented Ag–Cu ₂ O composited mesocrystals with efficient charge separation and transfer as well as visible light harvesting for enhanced photocatalytic activity. Nanoscale, 2021, 13, 11867-11877.	5.6	22
57	Hollow Cu _x O (x = 2, 1) micro/nanostructures: synthesis, fundamental properties and applications. CrystEngComm, 2017, 19, 6225-6251.	2.6	21
58	Formation of hierarchically polyhedral Cu7S4 cages from Cu2O templates and their structure-dependent photocatalytic performances. New Journal of Chemistry, 2013, 37, 3679.	2.8	20
59	A very facile strategy for the synthesis of ultrathin CuO nanorods towards non-enzymatic glucose sensing. New Journal of Chemistry, 2018, 42, 6364-6369.	2.8	20
60	An LSPR-based "push–pull―synergetic effect for the enhanced photocatalytic performance of a gold nanorod@cuprous oxide-gold nanoparticle ternary composite. Nanoscale, 2020, 12, 1912-1920.	5.6	20
61	Sulfate-ion-assisted galvanic replacement tuning of silver dendrites to highly branched chains for effective SERS. Physical Chemistry Chemical Physics, 2014, 16, 18918-18925.	2.8	19
62	Fe ₃ O ₄ Anisotropic Nanostructures in Hydrogels: Efficient Catalysts for the Rapid Removal of Organic Dyes from Wastewater. ChemPhysChem, 2016, 17, 1999-2007.	2.1	19
63	Twin engineering of photocatalysts: a minireview. Catalysis Science and Technology, 2020, 10, 4164-4178.	4.1	19
64	One-pot synthesis of etched Cu ₂ O cubes with exposed {110} facets with enhanced visible-light-driven photocatalytic activity. Physical Chemistry Chemical Physics, 2015, 17, 29479-29482.	2.8	18
65	One-pot construction of robust BiOCl/ZnO p–n heterojunctions with semi-coherent interfaces toward improving charge separation for photodegradation enhancement. Nanoscale Advances, 2021, 3, 4851-4857.	4.6	18
66	Enhanced photocatalytic property of hybrid graphitic C3N4 and graphitic ZnO nanocomposite: the effects of interface and doping. Journal of Physics Condensed Matter, 2018, 30, 175001.	1.8	17
67	Nanoparticle-aggregated octahedral copper hierarchical nanostructures. CrystEngComm, 2011, 13, 63-66.	2.6	16
68	Nanocube-aggregated cauliflower-like copper hierarchical architectures: synthesis, growth mechanism and electrocatalytic activity. CrystEngComm, 2012, 14, 5737.	2.6	16
69	Three-in-one to enhance visible-light driven photocatalytic activity of BiOCI: Synergistic effect of mesocrystalline stacking superstructure, porous nanosheet and oxygen vacancy. Journal of Materiomics, 2021, 7, 328-338.	5.7	16
70	Pyridine-containing block copolymer/silica core–shell nanoparticles for one-step preparation of superhydrophobic surfaces. Physical Chemistry Chemical Physics, 2013, 15, 10921.	2.8	15
71	Tuning Interfacial Cuâ€O Atomic Structures for Enhanced Catalytic Applications. Chemistry - an Asian Journal, 2019, 14, 2912-2924.	3.3	14
72	One-pot fabrication of novel cuboctahedral Cu ₂ O crystals enclosed by anisotropic surfaces with enhancing catalytic performance. Physical Chemistry Chemical Physics, 2014, 16, 20424-20428.	2.8	13

#	Article	IF	CITATIONS
73	One-pot construction of unprecedented direct Z-scheme ZnS/GaOOH heterojunction for photodegradation of antibiotics. Applied Surface Science, 2022, 576, 151742.	6.1	13
74	The electrochemical properties of Al–Si–Ni alloys composed of nanocrystal and metallic glass for lithium-ion battery anodes. Journal of Solid State Electrochemistry, 2012, 16, 2159-2167.	2.5	12
75	Magnetic field controlled particle-mediated growth inducing icker-like silver architectures. Chemical Engineering Journal, 2014, 240, 494-502.	12.7	12
76	Spatial charge separation and high-index facet dependence in polyhedral Cu ₂ O type-II surface heterojunctions for photocatalytic activity enhancement. Inorganic Chemistry Frontiers, 2021, 8, 2603-2610.	6.0	12
77	An Mn ²⁺ -mediated construction of rhombicuboctahedral Cu ₂ O nanocrystals enclosed by jagged surfaces for enhanced enzyme-free glucose sensing. CrystEngComm, 2020, 22, 2042-2048.	2.6	11
78	Designated-Tailoring on {100} Facets of Cu ₂ 0 Nanostructures: From Octahedral to Its Different Truncated Forms. Journal of Nanomaterials, 2010, 2010, 1-11.	2.7	8
79	Magnetic field driven assembly of 1D-aligned silver superstructures. CrystEngComm, 2011, 13, 4827.	2.6	8
80	Electrochemical deposition mediated growth of hierarchical Au architectures and the applications for SERS. CrystEngComm, 2012, 14, 656-662.	2.6	8
81	Copper-templated synthesis of gold microcages for sensitive surface-enhanced Raman scattering activity. RSC Advances, 2014, 4, 27074-27077.	3.6	7
82	Preparation of nanoporous Cu/Cu2O composites by anodic oxidation and their electrocatalytic performance towards methanol oxidation. Materials Today Communications, 2021, 26, 101992.	1.9	5
83	Water-guided synthesis of well-defined inorganic micro-/nanostructures. Chemical Communications, 2019, 55, 9418-9431.	4.1	4
84	Effect of thermal oxidation on microstructures and mechanical properties of nanoporous coppers. Science China Technological Sciences, 2018, 61, 1839-1844.	4.0	3
85	Monolithic Micro/Nanoporous Copper: Preparation, Mechanical and Electrocatalytic Properties. Materials Transactions, 2020, 61, 1045-1048.	1.2	3
86	Surface engraving engineering of polyhedral photocatalysts. Catalysis Science and Technology, 2021, 11, 6001-6017.	4.1	2
87	Porous/dense ZnO bilayer films grown by thermal oxidation of ZnS film with gallium. Vacuum, 2018, 153, 96-100.	3.5	1
88	First-principles Study of Crystal Structure Prediction, Electronic, Thermodynamic and Mechanical Properties of Al-Li Binary System. Materials Today Communications, 2021, , 102920.	1.9	1